Chemical Physics Letters 748 (2020) 137382

Contents lists available at ScienceDirect

Chemical Physics Letters

journal homepage: www.elsevier.com/locate/cplett

Research paper

Dissociation energy of the HCN···HF dimer

Thomas More Sexton, William Zeller Van Benschoten, Gregory S. Tschumper*

Department of Chemistry and Biochemistry, University of Mississippi, University, MS 38677-1848, United States

HIGHLIGHTS

- Discrepancy in experimental gas-phase dissociation energies resolved by computation.
- Computed anharmonic vibrational frequencies closely match experimental fundamentals.
- Computed vibrationally corrected geometry and dipole moment match experimental data.

ARTICLE INFO

Keywords:
Dissociation energy
Hydrogen bonded dimer
Theory-experiment benchmarking
Second order vibrational perturbation theory

ABSTRACT

Three different experimental dissociation energies (D_0) have been reported for the simple HCN···HF hydrogen bonded dimer, but none agree to within their error bars (4.42 ± 0.26, 4.96 ± 0.05, and 5.63 ± 0.03 kcal mol^{-1}). To help resolve this disagreement, the geometry, dipole moment, fundamental vibrational frequencies, and D_0 of the HCN···HF complex are computed with the CCSD(T) and MP2 methods and quintuple- quality basis sets, including anharmonic corrections from second-order vibrational perturbation theory. Our best estimate of D_0 = 5.56 kcal mol^{-1} lies within 0.07 kcal mol^{-1} of the largest experimental values, suggesting that neither of the older and smaller values based on equilibrium transition intensity measurements are reliable.

1. Introduction

The accuracy of quantum chemical methods can be determined by comparisons with higher level theory or by comparisons with experimental data [1]. Small molecule dimers are accurately measurable by experiment and computable by theory, thereby providing a fertile ground for developing this benchmarking process. Interest in this type of benchmarking is growing, and a database of small-molecule hydrogen bonds has been recently published,[2] with the authors inviting extensions in "chemical, observable, and quantum mechanical method space". Such an endeavor depends on accurate experimental and computational data for a variety of small molecule dimers. The heterodimer of HCN and HF (HCN-HF) is an excellent candidate for study by theory in this regard, due to extensive experimental investigation, including three measured values for the dissociation energy which do not agree within their error bars (*vide infra*). HF is commonly studied in prototypical hydrogen bonding systems, and HCN-HF has been extensively studied and reviewed up to 1986 [3] as a prototypical hydrogen bonded system for gas phase study. Here, we model HCN-HF with modern theoretical methods to resolve the disagreement in reported experimental dissociation energies and confirm other experimental measurements.

The heterodimer of HCN and HF was initially detected in gas phase in 1971 [4]. Although HF and HCN are both capable of acting as a hydrogen bond acceptor and as a hydrogen bond donor, only the complex with HCN as the hydrogen bond acceptor was found in the gas phase, denoted here as HCN···HF (Fig. 1b). Early computational studies examining both HCN···HF and the reversed complex HF···HCN (Fig. 1d) also found that HCN should be the hydrogen bond acceptor in the complex,[5] confirming the initial experimental findings. In the gas phase, the HCN···HF geometry is linear, with the N on HCN receiving a hydrogen bond from HF [6]. The heterodimer of HCN and HF has also been studied in liquid Xe,[7] solid Ar [8] and liquid He [9]. In addition to the HCN···HF complex, the reversed complex HF···HCN has been found in some condensed phase experiments, with HCN donating the hydrogen bond (Fig. 1d) [8,9]. However, the HF···HCN complex is metastable and easily converts to the linear HCN···HF complex when warmed or photoexcited [8,9]. In addition, preliminary computational investigations [10] have found HF···HCN to be 4.7 kcal mol^{-1} higher in energy than HCN···HF, with a barrier of approximately 1.5 kcal mol^{-1} for the HF···HCN → HCN···HF reaction. Because of the high relative energy and instability of the HF···HCN conformer, and because only the linear HCN···HF conformer is found in the gas phase, the analysis presented here will focus on the linear

* Corresponding author.
E-mail address: tschumpr@olemiss.edu (G.S. Tschumper).

https://doi.org/10.1016/j.cplett.2020.137382
Received 14 February 2020; Received in revised form 17 March 2020; Accepted 18 March 2020
Available online 24 March 2020

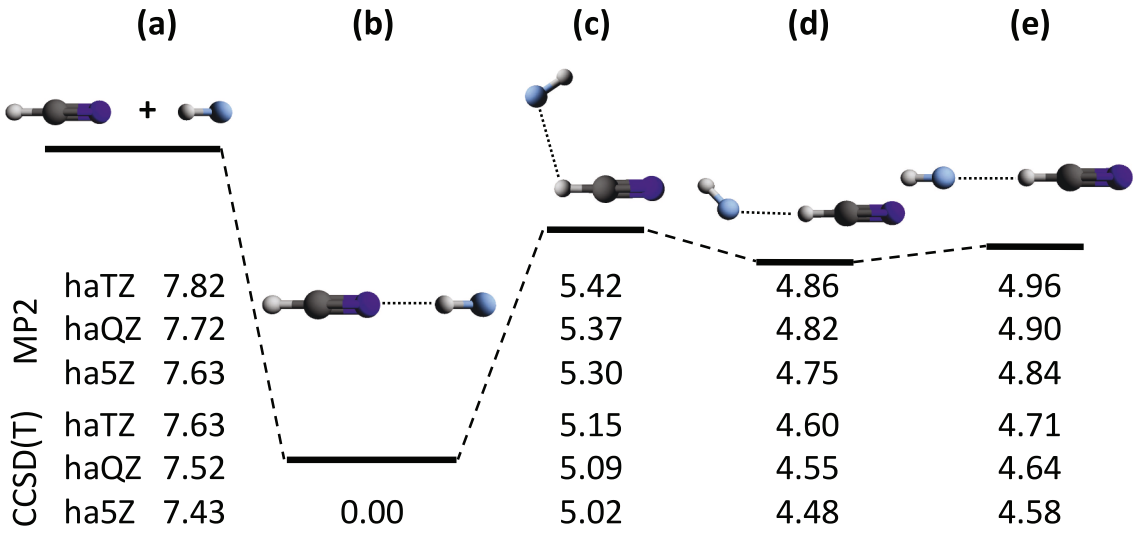

Fig. 1. Relative electronic energies (kcal mol^{-1}) with respect to the $C_{\infty v}$ global minimum HCN···HF (b) for dissociated monomers (a), the C_s Transition State connecting HF···HCN and HCN···HF (c), the C_s HF···HCN local minimum (d), and the $C_{\infty v}$ Second Order Saddle Point close to HF···HCN (e) at indicated method and basis.

HCN···HF conformer.

In the course of the aforementioned investigations, several observables were measured, including some which are particularly suitable for comparison with our computed results. The distance between N and F r_a(N···F) in gas phase HCN···HF was initially measured at 2.796 Å [6] and later updated to 2.8043 Å [11]. In both cases the rigid monomer approximation was used. The dipole moment of the linear HCN···HF complex has been measured experimentally in the gas phase (~5.6 D) [6,12] and in the condensed phase (5.8 D) [10]. The dipole moment enhancement in the gas phase (relative to the sum of monomer dipole moments) was found to be + 0.80 D [12]. All fundamental vibrational frequencies [13–17] have been measured for the HCN···HF complex in the gas phase.

Three experimental values for the dissociation energy D_0 of HCN···HF are available in the literature. The first experimental determination of D_0 was 4.42 ± 0.26 kcal mol^{-1} based on equilibrium transition intensity measurements of the complex in the gas phase [18]. Another experimental determination gave 4.96 ± 0.05 kcal mol^{-1} based on a similar experimental method [19]. Finally, an additional dissociation energy measurement based on vibrational predissociation gave D_0 = 5.63 ± 0.03 kcal mol^{-1} [20]. None of these experimental values for D_0 agree with the others to within their error bars. In addition to direct measurement, dissociation energies have been estimated by model potentials built on extensive experimental frequency data. One model potential derived D_0 of 5.83 kcal mol^{-1},[21] significantly higher than the same author's 4.96 kcal mol^{-1} experimental value [19]. Another model potential derived from experimental data gave D_e = 6.94 kcal mol^{-1}, although experimental D_0 values were used in developing that model [22]. More recently, Rivera-Rivera and Hren generated a potential for HCN···HF from experimental data, including Miller and Oudejans' D_0, which returned the same D_0 that was used to fit the potential.

At the time Miller and Oudejans' D_0 was published, no theoretical D_0 was available for HCN···HF with sufficient accuracy to discriminate between the experiments [20]. Since that time, additional authors have computed D_e values [23–27]. However, none of these included anharmonic ZPVE correction in an attempt to resolve the disconnect between available experimental values. The highest-level computed D_e available is 7.45 kcal mol^{-1} from a data set of D_e values for dimers computed by Boese of CCSD(T) energetics near the complete basis set limit, including contributions from core-valence and scalar relativistic effects [24]. However, Boese's study focused on theory benchmarking and did not examine zero-point contributions to the dissociation energy or compute other properties for comparison with experimental results.

When dissociation energies are computed via the supermolecular method, finite sized basis sets introduce an inconsistency commonly referred to as basis set superposition error or BSSE [28,29]. The counterpoise (CP) procedure can be used to evaluate the significance of BSSE on energies and geometries [30–32]. For the HCN···HF complex, the magnitude of the counterpoise correction to D_0 with double-ζ quality basis sets can be larger than the difference in energies between the experimental reported values for D_0. For example, Simon et al. [32] found a counterpoise correction of 1.31 kcal mol^{-1} for MP2/6-31G(d, p) and 2.48 kcal mol^{-1} for MP2/D95++(d, p). In contrast, the difference between the closest two previously mentioned experimental D_0 values is 0.7 kcal mol^{-1}. In addition, Simon *et al.* found that N···F distance computed by MP2/6-31G(d, p) changed by 0.083 Å with counterpoise correction, while intramolecular covalent bond distances were minimally effected (≲0.001 Å). Therefore, we will use larger basis sets to provide results accurate enough to compare to experimental values, and the convergence behavior of the counterpoise correction and the intermolecular distance will be monitored to determine closeness to the complete basis set limit.

For similar dimers, *ab initio* methods such using CCSD(T) with at least QZ quality basis sets for energies and harmonic frequencies and VPT2 anharmonic correction from MP2 have been successful at matching experimental fundamental frequencies and dissociation energies [33]. *Ab initio* methods have also been used to highlight discrepancies between experimental and theoretical dissociation energies [34]. In addition, anharmonic estimates based on VPT2 have been used to provide frequencies comparable to experiment [33–36]. In this work, a similar level of theory to the previous examples is employed to resolve the discrepancy in measured dissociation energies and to confirm the measured fundamental vibrational frequencies, geometries, and dipole moments.

2. Computational details

Full geometry optimizations were performed on HCN···HF (Fig. 1ab) and and its monomers using the CCSD(T) [37,38] and MP2 [39] methods with mixed basis sets ha*XZ* (cc-pV*XZ* on H and aug-cc-pV*XZ* on C, N, and F) where X = T, Q, 5 [40,41]. To assess the impact of diffuse functions on hydrogen, MP2 computations were also performed using Dunning's aug-cc-pV*YZ* basis sets, abbreviated as a*YZ*, where Y = T and Q. In each case, harmonic vibrational frequency computations

were performed to confirm HCN···HF and its monomers as minimum energy structures with no imaginary frequencies.

CCSD(T)/ha*XZ* and MP2/ha*XZ* (X = T, Q, 5) geometry optimizations were also performed on the reversed complex HF···HCN (Fig. 1d), the transition state which connects the two minima (Fig. 1c), and a second order saddle point found by forcing HF···HCN into a linear configuration (Fig. 1de). Harmonic vibrational frequency computations were performed on the MP2/ha*XZ* (X = T, Q, 5) and CCSD(T)/ha*YZ* (Y = T, Q) optimized geometries to confirm them as minima, transition states, or second order saddle points with zero, one, or two imaginary frequencies respectively. Although CCSD(T)/ha5Z optimized geometries were computed for HF···HCN, the transition state, and the second order saddle point, the corresponding CCSD(T)/ha5Z frequencies were skipped for cost considerations.

In addition, second order vibrational perturbation theory (VPT2) computations [42–45] were performed on HCN···HF and its monomers using MP2/ha*XZ* and CCSD(T)/haTZ. These computations allowed determination of equilibrium dissociation energy D_e , zero point vibrational energy (ZPVE) corrected dissociation energies D_0, harmonic and VPT2 vibrational frequencies, vibrationally averaged dipole moments $\langle\mu\rangle$, and distance between vibrationally averaged atomic positions r_a.

Gradients and Hessians were computed analytically. Force constants for VPT2 were computed numerically from finite differences of analytic second derivatives [46]. The 1*s* character core orbitals were frozen on C, N, and F in the MP2 and CCSD(T) computations. To examine the significance of BSSE [28,29] for these systems, the electronic dissociation energies were computed for HCN···HF using the CP procedure [30,31]. Results of the CP computations are summarized in the Supplementary Material. All computations were performed in the CFOUR package [47].

3. Results and discussion

The first part of this section discusses the geometry and properties of four stationary points found on the HCN-HF potential energy surface. VPT2 computations on the global minimum of the HCN···HF complex allow direct comparison with the available experimental dipole moment, geometry data and the fundamental vibrational frequencies to evaluate the accuracy of the theoretical treatment of anharmonic effects for this system. Finally, the computed dissociation energies of HCN···HF are presented and discussed, including a composite D_0 of sufficient accuracy to resolve the discrepancy between published experimental D_0 values.

3.1. Stationary points and relative energies

Fig. 1 provides a schematic of the isolated HCN and HF monomers (Fig. 1a) and and the four stationary points of the HCN-HF complex (Fig. 1b-1e) investigated along with their relative electronic energies computed with the CCSD(T) and MP2 methods utilizing the ha*XZ* family of basis sets (X = T, Q, 5). Cartesian coordinates of optimized structures and details on convergence of geometric parameters with the MP2 and CCSD(T) methods and various correlation consistent basis sets are in the Supplementary Material. The only complex observed in the gas phase is the linear HCN···HF global minimum with $C_{\infty v}$ symmetry (Fig. 1b). The best gas phase experimental geometric parameter of HCN···HF available for comparison with our calculations is the distance between the average N and F positions, r_a(N···F). Experimental values for r_a(N···F) are based on the rigid monomer approximation and range from 2.796 Å [6] to 2.8043 Å [11]. In order to compare computational and experimental values, vibrational averaging is included in the computational model via VPT2. Our anharmonic estimate for r_a(N···F), using r_e of 2.781 Å from CCSD(T)/ha5Z with vibrational averaging correction of 0.026 Å from MP2/ha5Z, provides r_a(N···F) at 2.807 Å, in line with experimental values. Vibrationally averaged dipole moment $\langle\mu\rangle$ = 5.63 D and dipole moment enhancement on complexation $\Delta\langle\mu\rangle$ = +0.80 D for HCN···HF computed with CCSD(T)/haTZ also line up well with experimental values ($\langle\mu\rangle_{exp}$ = 5.612 D [12] and $\Delta\langle\mu\rangle_{exp}$ = +0.80 D [12]), giving further support to the computed geometry and the use of the VPT2 model for vibrationally averaged parameters for this system. Additional details on the dipole moment computations are included in the Supplementary Material.

The non-linear HF···HCN complex with C_s symmetry in which the hydrogen bond donor/acceptor roles are reversed (Fig. 1d) is 4.48 kcal mol^{-1} above HCN···HF according to CCSD(T)/ha5Z electronic energies, consistent with the experimental finding that HF···HCN is not seen in the gas phase. The C_s transition state connecting these minima (Fig. 1c) was also characterized. The CCSD(T)/ha5Z electronic barrier for the isomerization from this high-energy local minimum back to the global minimum (i.e., HF···HCN → HCN···HF) is 0.54 kcal mol^{-1}. This low barrier is consistent with the experimental observation that when HF···HCN is formed in low-temperature helium nanodroplets [9] or a solid Ar matrix [8], it is easily converted to HCN···HF upon photoexcitation or warming, respectively. Finally, a linear second order saddle point (Fig. 1e) is located only 0.10 kcal mol^{-1} above the nearby HF···HCN minimum at the CCSD(T)/ha5Z level of theory. This second order saddle point has two degenerate imaginary frequencies dominated by HFH bending, connecting equivalent forms of the HF···HCN local minimum.

Table 1
Harmonic vibrational frequencies (in cm^{-1}) for HCN···HF and the corresponding anharmonic corrections and estimates from VPT2, compared to gas phase experimental data.

	harmonic		ΔVPT2 correction				VPT2		
	MP2 ha5Z	CCSD(T) ha5Z	CCSD(T) haTZ	MP2 haTZ	MP2 haQZ	MP2 ha5Z	CCSD(T) haTZ	best est.[a]	Exp
ν_1	3843	3889	−161	−163	−168	−169	3719	3720	3716[b]
ν_2	3464	3437	−128	−125	−127	−128	3296	3309	3310[b]
ν_3	2071	2155	−35	−40	−40	−40	2105	2116	2121[b]
ν_4	188	185	−9	−9	−11	−11	176	174	168[c]
ν_5^1	738	737	−14	−10	−8	−9	718	729	727[b]
ν_6^1	641	626	−79	−76	−68	−69	554	557	550[d]
ν_7^1	79	80	−7	−7	−8	−5	76	75	76[e]

[a] CCSD(T)/ha5Z harmonic frequencies with MP2/ha5Z anharmonic correction.
[b] Ref. [16].
[c] Ref. [14].
[d] Ref. [15].
[e] Ref. [13].

3.2. Vibrational frequencies

Frequency data for the HCN···HF complex are aggregated in Table 1. The first two columns of data in Table 1 show the harmonic vibrational frequencies computed with the MP2 and CCSD(T) methods and the ha5Z basis set. For each method, the haQZ and ha5Z harmonic frequencies differ by less than 4 cm^{-1}, showing that MP2 and CCSD(T) harmonic frequencies and harmonic zero point energy corrections are both well converged at ha5Z. (See Supplementary Material for MP2/haQZ and CCSD(T)/haQZ frequencies.) Although both are near their complete basis set (CBS) limits, MP2 and CCSD(T) give quite different results for some modes, with MP2/ha5Z predicting the CN stretch ν_3 84 cm^{-1} below the value computed by CCSD(T)/ha5Z.

The next four columns of data in Table 1 show the anharmonic frequency corrections for CCSD(T)/haTZ and for MP2 at different basis set cardinality. The VPT2 corrections never differ by more than 5 cm^{-1} between CCSD(T)/haTZ and MP2/haTZ, justifying the use of MP2 for anharmonic frequency correction. As MP2 is less computationally demanding than CCSD(T), the MP2 VPT2 corrections are computed up to MP2/ha5Z. The MP2/haQZ and MP2/ha5Z anharmonic corrections never differ by more than 1 cm^{-1}, indicating that basis set convergence has been reached for anharmonic correction at MP2/ha5Z.

The seventh column of data in Table 1 shows the fundamental frequencies computed with CCSD(T)/haTZ. These values differ from experimental gas phase frequencies (last column of data) by up to 9 cm^{-1} for the intermolecular modes and up to 16 cm^{-1} for the intramolecular modes. An improved anharmonic estimate is generated when MP2/ha5Z anharmonic corrections are used with CCSD(T)/ha5Z harmonic frequencies. This anharmonic estimate differs from experimental values by at most 7 cm^{-1} for the intermolecular modes and at most 5 cm^{-1} for the intramolecular modes, showing that this composite VPT2 model captures the anharmonic effects for this system reasonably well.

3.3. Dissociation energies

Table 2 contains the dissociation energies and related terms computed at the MP2 and CCSD(T) levels of theory. The final rows of Table 2 show the experimental values for D_0. The two experimental values with the smallest error bars (± 0.05 and ± 0.03 kcal mol^{-1}) still differ by 0.67 kcal mol^{-1}. The first column of data shows the computed electronic dissociation energy D_e . Even at ha5Z, which should be close to the complete basis set limit for both methods, CCSD(T) and MP2 differ in D_e by 0.20 kcal mol^{-1}, indicating a significant effect from higher-order electron correlation.

CCSD(T)/ha5Z gives D_e of 7.43 kcal mol^{-1}, identical to the extrapolated CBS limit found by Boese [24] based on a two point CCSD(T)/a{Q,5}Z extrapolation with corrections for additional effects, such as relativistic and core-valence correlation. It is also close to a composite best estimate of 7.45 kcal mol^{-1} found by the same author when including additional corrections beyond CCSD(T). These results indicate that our values obtained with the ha5Z basis set are very close to the CBS limit where BSSE vanishes by definition. Consequently, dissociation energies computed with the CP procedure have been relegated to the Supplementary Material.

The second and third columns of data in Table 2 show how the harmonic zero point vibrational energy changes the dissociation energy (δZPVE) as well as the resulting dissociation energy (D_0) that includes the harmonic ZPVE. As noted previously, MP2/ha5Z and CCSD(T)/ha5Z give substantially different harmonic frequencies for HCN···HF which leads to harmonic zero point vibrational energies of the complex that differ by roughly 0.1 kcal mol^{-1}. However, a similar effect for monomers leads to a fortuitous cancellation, and MP2 and CCSD(T) give similar harmonic δZPVE values for the overall reaction. In any case, δZPVE is remarkably consistent between MP2 and CCSD(T) near − 2.00 kcal mol^{-1}, regardless of basis set size.

The corresponding anharmonic values from VPT2 computations are given in the last two columns of data in Table 2. The VPT2 treatment only decreases the magnitude of the ZPVE corrections by 0.13 to 0.17 kcal mol^{-1}, which ultimately leads to slightly larger dissociation energies. This anharmonic correction to δZPVE and D_0 is similar to that obtained for the closely related H_2O···HF system for which the change is roughly twice as large [34]. A Fermi resonance is present [48] in HCN···HF between $2\nu_7$ and ν_4, but its treatment is neglected because these intermolecular modes have only a small effect on the anharmonic zero point vibrational energy and corresponding D_0.

The final column of data in Table 2 shows the computed anharmonic dissociation energy for each level of theory. The same composite scheme used to obtain accurate anharmonic vibrational frequencies in Table 1 is adopted here for the anharmonic ZPVE data in Table 2. Therefore, our best anharmonic estimate of D_0 = 5.56 kcal mol^{-1} is constructed from the CCSD(T)/ha5Z harmonic D_0 (5.43 kcal mol^{-1}) and an anharmonic correction of + 0.13 kcal mol^{-1} from the MP2/ha5Z VPT2 computation.

The final three rows of Table 2 contain D_0 values based on experimental measurements. Even the computed harmonic D_0 values suggest the dissociation energy of 5.63 kcal mol^{-1} measured by vibrational predissociation [20] is correct. Anharmonic corrections further improve agreement with that experimental D_0, with our best estimate of D_0 giving a deviation of only 0.07 kcal mol^{-1} between experiment and theory. The other experimental values, based on equilibrium intensity measurements from Ref [19,18], deviate by at least 0.60 kcal mol^{-1} from all of our anharmonic estimates.

With experiment and theory having converged on a D_0 for the mixed HCN···HF dimer near 5.6 kcal mol^{-1}, it is interesting to note that this value is significantly larger than D_0 for either of the corresponding homogeneous dimers (ca. 3.0 kcal mol^{-1} for $(HF)_2$ and 3.9 kcal mol^{-1} for $(HCN)_2$) [33,49,50]. An analogous result is seen for the dimers of H_2O and HF where D_0 for the heterogeneous H_2O···HF dimer (ca. 6.2 kcal mol^{-1}) [34] is approximately twice that of either homogeneous dimer (⩽3.1 kcal mol^{-1} for $(H_2O)_2$ and $(HF)_2$).

Table 2
MP2 and CCSD(T) dissociation energies (D_e and D_0 in kcal mol^{-1}) and zero point vibrational energy corrections (δZPVE in kcal mol^{-1}) based on the harmonic approximation or anharmonic values from VPT2, for the HCN···HF complex.

		harmonic		VPT2	
	D_e	δZPVE	D_0	δZPVE	D_0
MP2/haTZ	7.82	−2.03	5.79	−1.88	5.94
MP2/haQZ	7.72	−2.01	5.70	−1.88	5.84
MP2/ha5Z	7.63	−1.99	5.64	−1.86	5.77
CCSD(T)/haTZ	7.63	−2.05	5.58	−1.89	5.74
CCSD(T)/haQZ	7.52	−2.03	5.40	−1.90[a]	5.62[a]
CCSD(T)/ha5Z	7.43	−2.00	5.43	−1.87[a]	5.56[a]
Experimental Ref. [18], equilibrium transition intensity					4.42 ± 0.26
Experimental Ref. [19], equilibrium transition intensity					4.96 ± 0.05
Experimental Ref. [20], vibrational predissociation					5.63 ± 0.03

[a]using MP2/ha5Z anharmonic correction of + 0.13 kcal mol^{-1}.

4. Conclusions

The linear HCN···HF global minimum in which HCN accepts a hydrogen bond from HF has been examined with the CCSD(T) method and large basis sets, along with the C_s HF···HCN local minimum in which the donor/acceptor roles have been reversed, and the transition state connecting them. Several properties of the experimentally relevant HCN···HF complex have been computed, with good alignment with

experimental data. Our anharmonic estimate for the distance between the average N and F positions, r_a(N···F) = 2.807 Å, is within 0.02 Å of experimental values. In addition, CCSD(T)/haTZ with VPT2 gives vibrationally averaged dipole moment $\langle\mu\rangle$ = 5.63 D and dipole moment enhancement on complexation $\langle\mu\rangle$ = + 0.80 D both within 0.02 D of experimental values. The fundamental frequencies computed from CCSD(T)/ha5Z harmonic frequencies and MP2/ha5Z anharmonic correction differ from experimental frequencies by at most 7 cm^{-1}. Finally, an anharmonic estimate for D_0 = 5.56 kcal mol^{-1} has been computed, close to the most recent experimental value of 5.63 kcal mol^{-1} from Oudejans and Miller determined by vibrational predissociation [20]. As the older equilibrium transition intensity measurements [18,19] have approximately an order of magnitude larger deviation from our anharmonic estimate, vibrational predissociation likely provides the best currently available experimental value of D_0 for this small and relatively simple hydrogen bonded dimer. Given the encouraging results obtained here for the HCN···HF dimer, the computational analysis employed in this work will be extended to closely related hydrogen halide analogues such as HCN···HCl and HCN···HBr.

CRediT authorship contribution statement

Thomas More Sexton: Conceptualization, Investigation, Data curation, Writing - original draft, Writing - review & editing. **William Zeller Van Benschoten:** Investigation, Data curation. **Gregory S. Tschumper:** Conceptualization, Resources, Writing %E2%80%93 review %26_editing, Supervision, Funding acquisition.

Declaration of Competing Interest

The authors declare that they have no known competing financial interests or personal relationships that could have appeared to influence the work reported in this paper.

Acknowledgments

Supported under the Nation Science Foundation, Grant Nos. CHE-1460568 and CHE-1664998. The Mississippi Center for Supercomputing Research is thanked for a generous allotment of computer time.

Appendix A. Supplementary material

Supplementary data associated with this article can be found, in the online version, at https://doi.org/10.1016/j.cplett.2020.137382.

References

[1] R.A. Mata, M.A. Suhm, Benchmarking quantum chemical methods: are we heading in the right direction? Angew. Chem. Int. Ed. 56 (2017) 11011–11018.
[2] S. Oswald, M.A. Suhm, Soft experimental constraints for soft interactions: a spectroscopic benchmark data set for weak and strong hydrogen bonds, Phys. Chem. Chem. Phys. 21 (2019) 18799–18810.
[3] A.C. Legon, D.J. Millen, Gas-phase spectroscopy and the properties of hydrogen-bonded dimers: HCN···HF as the spectroscopic prototype, Chem. Rev. 86 (1986) 635–657.
[4] R.K. Thomas, Hydrogen bonding in the gas phase: the infrared spectra of complexes of hydrogen fluoride with hydrogen cyanide and methyl cyanide, Proc. R. Soc. Lond. A 325 (1971) 133–149.
[5] A. Johansson, P. Kollman, S. Rothenberg, Hydrogen bonding and the structure of the HF-HCN dimer, Chem. Phys. Lett. 16 (1972) 123–127.
[6] A.C. Legon, D.J. Millen, S.C. Rogers, Dipole moment enhancement on formation of a hydrogen-bonded complex. demonstration and measurement of the effect for HCN···HF by microwave spectroscopy, Chem. Phys. Lett. 41 (1976) 137–138.
[7] K. Tokhadze, N. Dubnova, Z. Mielke, M. Wierzejewska-Hnat, H. Ratajczak, The evolution of the ν_{HF} band of weak HCN…HF, CH_3N…HF complexes on transition from gas to liquid state, Chem. Phys. Lett. 202 (1993) 87–92.
[8] G.L. Johnson, L. Andrews, Infrared spectra of two 1: 1 complexes between HCN and HF in solid argon at 12K.J, Am. Chem. Soc. 105 (1983) 163–168.
[9] G.E. Douberly, J.M. Merritt, R.E. Miller, IR-IR double resonance spectroscopy in helium nanodroplets: photo-induced isomerization, Phys. Chem. Chem. Phys. 7 (2005) 463–468.
[10] G.E. Douberly, R.E. Miller, The isomers of HF-HCN formed in helium nanodroplets: infrared spectroscopy and abinitio calculations, J. Chem. Phys. 122 (2005) 024306.
[11] A.C. Legon, D.J. Millen, L.C. Willoughby, Spectroscopic investigations of hydrogen bonding interactions in the gas phase. X. Properties of the hydrogen-bonded heterodimer HCN···HF determined from hyperfine coupling and centrifugal distortion effects in its ground-state rotational spectrum, Proc. R. Soc. Lond. A 401 (1985) 327–347.
[12] A.C. Legon, D.J. Millen, S.C. Rogers, The electric dipole moment of the hydrogen-bonded heterodimer HCN···HF. An investigation of the conditions leading to inadequacy of the second- and fourth-order perturbation theories of the stark effect for linear molecules, J. Mol. Spectry. 70 (1978) 209–215.
[13] J.W. Bevan, Dynamical properties of simple hydrogen-bonded clusters, Struct. Dyn. Weakly Bonded Mol. Complexes 212 (1987) 149–169.
[14] D. Bender, M. Eliades, D.A. Danzeiser, M.W. Jackson, J.W. Bevan, The gas phase infrared spectrum of ν_1 and ν_1-ν_4 HCN-HF, J. Chem. Phys. 86 (1987) 1225–1234.
[15] B.A. Wofford, M.W. Jackson, J.W. Bevan, W.B. Olson, W.J. Lafferty, Rovibrational analysis of an intermolecular hydrogen-bonded vibration: The ν_6^1 band of HCN-HF, J. Chem. Phys. 84 (1986) 6115–6118.
[16] B.A. Wofford, J.W. Bevan, W.R. Olson, W.J. Lafferty, Rovibrational analysis of the ν_5^1 Band in the HCN-HF hydrogen bonded cluster, Chem. Phys. Lett. 124 (1986) 579–582.
[17] B.A. Wofford, J.W. Bevan, W.B. Olson, W.J. Lafferty, Rovibrational analysis of ν_3 HCN-HF using Fourier transform infrared spectroscopy, J. Chem. Phys. 83 (1985) 6188–6192.
[18] A.C. Legon, D.J. Millen, P.J. Mjöberg, S.C. Rogers, A method for the determination of the dissociation energies D_0 and D_e for hydrogen-bonded dimers from the intensities of rotational transitions and its application to HCN···HF, Chem. Phys. Lett. 55 (1978) 157–159.
[19] B.A. Wofford, M.E. Eliades, S.G. Lieb, J.W. Bevan, Determination of dissociation energies and thermal functions of hydrogen- bond formation using high resolution FTIR spectroscopy, J. Chem. Phys. 87 (1987) 5674–5680.
[20] L. Oudejans, R.E. Miller, Mode dependence of the state-to-state vibrational dynamics of HCN-HF, Chem. Phys. 239 (1998) 345–356.
[21] A. McIntosh, A.M. Gallegos, R.R. Lucchese, J.W. Bevan, The validity of the hard-sphere model in hydrogen bonded intermolecular interactions of HCN-HF, J. Chem. Phys. 107 (1997) 8327–8337.
[22] A. Quinones, G. Bandarage, J.W. Bevan, R.R. Lucchese, Inversion of experimental data and *ab initio* studies of a pseudo- atom-diatom model for the vibrational dynamics of HCN-HF, J. Chem. Phys. 97 (1992) 2209–2223.
[23] M. Domagala, S.J. Grabowski, X-H···π and X-H···N hydrogen bonds - acetylene and hydrogen cyanide as proton acceptor, Chem. Phys. 363 (2009) 42–48.
[24] A.D. Boese, Assessment of coupled cluster theory and more approximate methods for hydrogen bonded systems, J. Chem. Theory Comput. 9 (2013) 4403–4413.
[25] I. Alkorta, A.C. Legon, Nucleophilicities of lewis bases B and electrophilicities of lewis acids a determined from the dissociation energies of complexes B···A involving hydrogen bonds, tetrel bonds, pnictogen bonds, chalcogen bonds and halogen bonds, Molecules 22 (2017) 1786.
[26] L.A. Rivera-Rivera, Z.R. Hren, Compound-model morphed potential for the hydrogen bond HCN···HF, Mol. Phys. 117 (2019) 539–546.
[27] L.A. Terrabuio, W.E. Richter, A.F. Silva, R.E. Bruns, R.L.A. Haiduke, An atom in molecules study of infrared intensity enhancements in fundamental donor stretching bands in hydrogen bond formation, Phys. Chem. Chem. Phys. 16 (2014) 24920.
[28] N.R. Kestner, He-He interaction in the SCF-MO approximation, J. Chem. Phys. 48 (1968) 252–257.
[29] B. Liu, A.D. McLean, Accurate calculation of the attractive interaction of two ground state helium atoms, J. Chem. Phys. 59 (1973) 4557–4558.
[30] H.B. Jansen, P. Ros, Non-empirical molecular orbital calculations on the protonation of carbon monoxide, Chem. Phys. Lett. 3 (1969) 140–143.
[31] S.F. Boys, F. Bernardi, The calculation of small molecular interactions by the differences of separate total energies. Some procedures with reduced errors, Mol. Phys. 19 (1970) 553–566.
[32] S. Simon, M. Duran, How does basis set superposition error change the potential surfaces for hydrogen-bonded dimers? J. Chem. Phys. 105 (1996) 11024–11031.
[33] J.C. Howard, J.L. Gray, A.J. Hardwick, L.T. Nguyen, G.S. Tschumper, Getting down to the fundamentals of hydrogen bonding: anharmonic vibrational frequencies of $(HF)_2$ and $(H_2O)_2$ from ab initio electronic structure computations, J. Chem. Theory Comput. 10 (2014) 5426–5435.
[34] T.M. Sexton, J.C. Howard, G.S. Tschumper, Dissociation energy of the H_2O···HF dimer, J. Phys. Chem. A 122 (2018) 4902–4908.
[35] S.N. Johnson, G.S. Tschumper, Hydrogen bonding in the Mixed HF/HCl dimer: is it better to give or receive, J. Comput. Chem. 39 (2018) 839–843.
[36] K.M. Dreux, G.S. Tschumper, Examination of the structures, energetics, and vibrational frequencies of small sulfur-containing prototypical dimers, $(H_2S)_2$ and H_2O/H_2S, J. Comput. Chem. 40 (2019) 231–238.
[37] R.J. Bartlett, Coupled-cluster theory and its equation-of-motion extensions, WIREs Comput. Mol Sci. 2 (2012) 126–138.
[38] K. Raghavachari, G.W. Trucks, J.A. Pople, M. Head-Gordon, A fifth-order perturbation comparison of electron correlation theories, Chem. Phys. Lett. 157 (1989) 479–483.
[39] C. Møller, M.S. Plesset, Note on an approximation treatment for many-electron systems, Phys. Rev. 46 (1934) 618–622.
[40] T.H. Dunning, Gaussian basis sets for use in correlated molecular calculations. I. The atoms boron through neon and hydrogen, J. Chem. Phys. 90 (1989) 1007–1023.

[41] R.A. Kendall, T.H. Dunning, R.J. Harrison, Electron affinities of the first-row atoms revisited. Systematic basis sets and wave functions, J. Chem. Phys. 96 (1992) 6796–6806.
[42] V. Barone, Anharmonic vibrational properties by a fully automated second-order perturbative approach, J. Chem. Phys. 122 (2005) 014108-1–014108-10.
[43] V. Barone, J. Bloino, C.A. Guido, F. Lipparini, A fully automated implementation of VPT2 infrared intensities, Chem. Phys. Lett. 496 (2010) 157–161.
[44] J. Vázquez, J.F. Stanton, Simple(r) algebraic equations for transition moments of fundamental transitions in vibrational second-order perturbation theory, Mol. Phys. 104 (2006) 377–388.
[45] I. Mills, N. Rao, C. Mathews (Eds.), Molecular Spectroscopy: Modern Research, vol. 1, Academic Press, New York, 1972, pp. 115–140.
[46] W. Schneider, W. Thiel, Anharmonic force fields from analytic second derivatives: method and application to methyl bromide, Chem. Phys. Lett. 157 (1989) 367–373.
[47] J.F. Stanton, J. Gauss, M.E. Harding, Szalay, P.G. Cfour, Coupled-Cluster techniques for Computational Chemistry. with contributions from A.A. Auer and R.J. Bartlett and U. Benedikt and C. Berger and D.E. Bernholdt and Y.J. Bomble and L. Cheng and O. Christiansen and M. Heckert and O. Heun and C. Huber and T.-C. Jagau and D. Jonsson and J. Jusélius and K. Klein and W.J. Lauderdale and D.A. Matthews and T. Metzroth and L.A. Mück and D.P. O'Neill and D.R. Price and E. Prochnow and K. Ruud and F. Schiffmann and W. Schwalbach and S. Stopkowicz and A. Tajti and J. Vázquez and F. Wang and J.D. Watts and the integral packages MOLECULE (J. Almlöf and P.R. Taylor) and PROPS (P.R. Taylor) and ABACUS (T. Helgaker and H. J. Aa. Jensen and P. Jørgensen and J. Olsen) and ECP routines by A.V. Mitin and C. van Wüllen. For the current version see http://www.cfour.de.
[48] A. Mclntosh, A. Gallegos, R. Lucchese, J. Bevan, A Fermi resonance study in $H^{12}C^{14}N$-$H^{19}F$ based on gas phase far infrared spectroscopy, J. Mol. Struct. 413–414 (1997) 167–173.
[49] J. Huang, D. Yang, Y. Zhou, D. Xie, A new full-dimensional *ab initio* intermolecular potential energy surface and vibrational states for $(HF)_2$ and $(DF)_2$, J. Chem. Phys. 150 (2019) 154302-1–154302-10.
[50] D. Mihrin, P.W. Jakobsen, A. Voute, L. Manceron, R.W. Larsen, High-resolution infrared synchrotron investigation of $(HCN)_2$ and a semi-experimental determination of the dissociation energy D_0, ChemPhysChem 20 (2019) 3238–3244.